Simulations of Finite β Turbulence in Tokamaks and Stellarators

F. Jenko, B. Scott, W. Dorland†, A. Kendl, D. Strintzi
Max-Planck-Institut für Plasmaphysik, EURATOM Association, 85748 Garching, Germany
† IREAP, University of Maryland, College Park, Maryland 20742, USA

Abstract

One of the central open questions in our attempt to understand microturbulence in fusion plasmas concerns the role of finite β effects. Nonlinear codes trying to investigate this issue must go beyond the commonly used adiabatic electron approximation - a task which turns out to be a serious computational challenge. This step is necessary because the passing electrons are the prime contributor to the parallel currents which in turn produce the magnetic field fluctuations. Results at both ion and electron space-time scales from gyrokinetic and gyrofluid models are presented which shed light on the character of finite β turbulence in tokamaks and stellarators.

1. Ion scales

Here, "ion scales" refers to scales of the order of ρ_i and somewhat larger, but still small compared to global scales. This comprises, in principle, electron drift waves, ion temperature gradient (ITG) modes, resistive ballooning modes, and their respective turbulence. In this section, we focus on core ITG turbulence which is traditionally studied in the adiabatic electron limit (cf. Ref. [1] and references therein). Using Landau fluid simulations, our primary interest is the effect of a finite plasma beta on ITG turbulence, and this necessarily requires a self-consistent electron treatment as in the earlier collisional drift wave turbulence models.[2, 3] In the latter case, finite β turns drift waves into drift Alfvén waves by making the adiabatic response of the electrons electromagnetic.[4] This, of course, also effects the turbulence.[5] Drift wave and ITG turbulence occur typically at frequencies of $(0.1-1)\,c_s/L_T$ and perpendicular wavenumbers of $(0.1-1)\,k_\perp\rho_s$, where $c_s^2 = T_e/m_i$, $\rho_s = c_s/\Omega_i$, and L_T is the temperature gradient scale length. This is to be compared to the electron and Alfvén transit frequencies, v_{te}/qR and v_A/qR respectively, where $v_{te}^2 = T_e/m_e$ and $v_A^2 = B^2/4\pi n_e m_i$, and $1/qR$ is the wavenumber associated with the field line connection length. The salient parameter for an electromagnetic electron response is $\hat{\beta} = (c_s/L_T)^2(qR/v_A)^2$, the drift Alfvén parameter. At zero beta, the salient parameter for a nonadiabatic electron response is $\hat{\mu} = (c_s/L_T)^2(qR/v_{te})^2$, which for finite β remains a measure for the importance of electron Landau damping. In the Ohm's law, electron inertia competes with electromagnetic induction, which due to Ampère's law incorporates two factors of $k_\perp\rho_s$. Hence, electromagnetic effects change the electron dynamics not only for $\hat{\beta}/\hat{\mu} > 1$, but already for $\hat{\beta}/\hat{\mu} > (k_\perp\rho_s)^2$, that is, for practically any situation of interest in tokamak plasmas, even in the edge. Electromagnetic effects enter the general dynamics whenever $\hat{\beta}$ is close to or larger than unity, a situation for which what is called the "Cyclone base case" is marginal (cf. Ref. [1]; the profile information needed for nonadiabatic electrons is available at `http://www.er.doe.gov/production/cyclone/`).

Edge turbulence, which does not concern us here, is treated elsewhere. Key results include the role of the drift wave nonlinear instability [3], its relationship to strongly electromagnetic ITG turbulence [6], and the competition between drift wave and resistive ballooning turbulence.[7] These studies found that it is imperative to diagnose the energetics in the context of the fully developed turbulence. Core turbulence, on the other hand, may be defined as the parameter regime in which $\hat{\mu} < 1$. For the Cyclone base case, the salient parameters are $\hat{\beta} = 0.464$

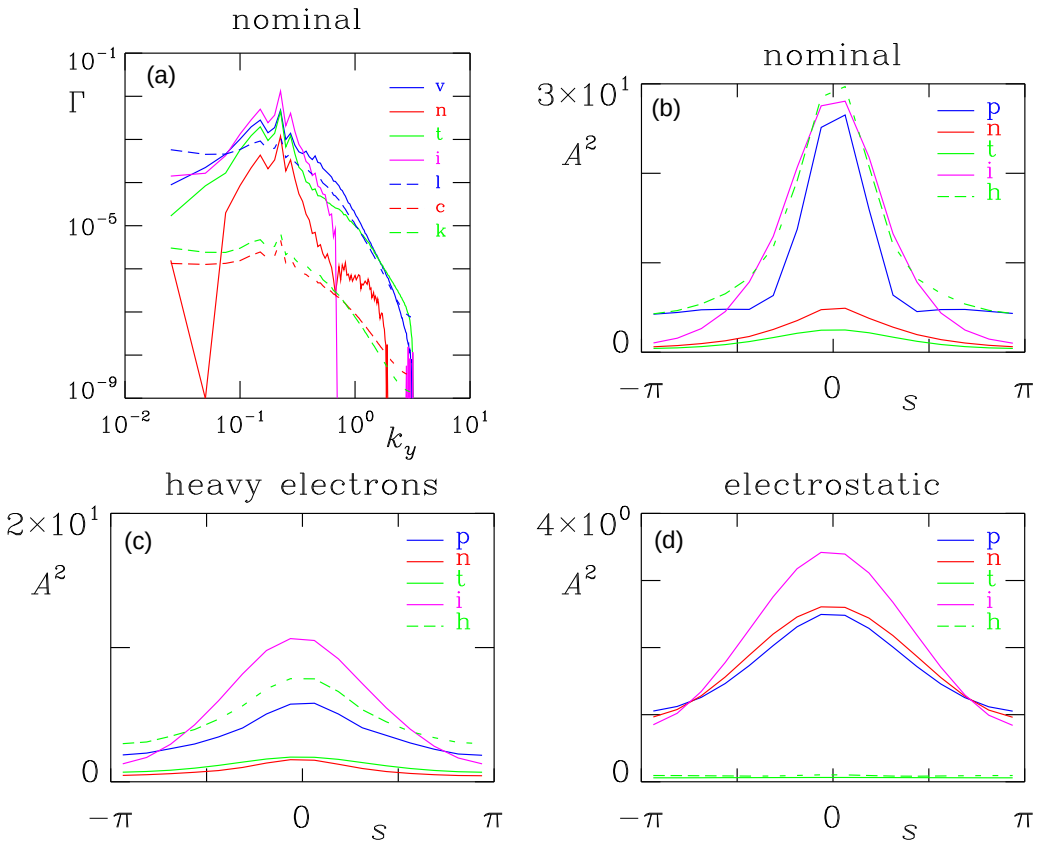

Figure 1: (a) Electromagnetic ITG source (solid lines) and sink (dashed) spectra for the Cyclone Base Case. The contributions are magnetic transport by electrons ('v'), ExB fluxes of density ('n'), electron ('t') and ion ('i') temperatures, Landau damping ('l'), and collisional resistivity ('c') and thermal conduction ('k'). (b) The corresponding parallel envelopes of the square amplitudes of $\widetilde{\phi}$ ('p'), $\widetilde{n}_e$ ('n'), $\widetilde{T}_e$ ('t'), $\widetilde{T}_i$ ('i') and the nonadiabatic $\widetilde{h}_e$ ('h'). (c) Parallel envelopes in the "electrostatic" case, and (d) in the case with a mass ratio $m_i/m_e = 450$.

and $\hat{\mu} = 0.0254$, and also the (very low) collisionality, $\hat{\nu} = \nu_e L_T/c_s = 0.033$. The other nominal parameters are chosen as in Ref. [1]: $2L_T/R = 0.29$, $\hat{s} = 0.78$, $L_T/L_n = 0.321$, $m_i/m_e = 3670$, and $T_i/T_e = 1$ for the background. For a baseline comparison, the warm ion Landau fluid model DALFTI [8] was run at these parameters and also for a companion case with $\hat{\beta} = 0.03$, which we call "electrostatic." The nominal grid was 256×256 for the perpendicular drift plane with an anisotropic resolution of $4\,h_x = h_y = \rho_s$. This is required to resolve every rational surface in the spectrum to avoid spurious electron grid modes. For the parallel direction, 16 drift planes within a single poloidal connection length were used. The geometry was a flux tube model with globally consistent boundary conditions [9], using a shifted metric procedure to represent slab and toroidal eigenmode types equally well [10].

In both cases, the turbulence is nonlinearly driven in a fairly narrow region in k_y space, weakly coupled to a wider bath of stable modes (see the source/sink spectra shown in Fig. 1a for the nominal case). The transport is very (even qualitatively) different, however: Q_i is twice as large in the nominal case with $Q_e = 0.6\,Q_i$, while in the "electrostatic" case, Q_e was indeed negligible owing to the generally adiabatic character. In the nominal case, the transport by electrons moving along disturbed magnetic field lines ("magnetic flutter") was also substantial, so that the total electron heat flux was about the same as the ion one. We also find significant differences in the mode structure (Figs. 1b and 1d for the nominal and low beta cases). Electron nonadiabaticity is represented by finite $\widetilde{T}_e$ and $\widetilde{h}_e = \widetilde{n}_e - \widetilde{\phi}$, which is robustly enabled by the

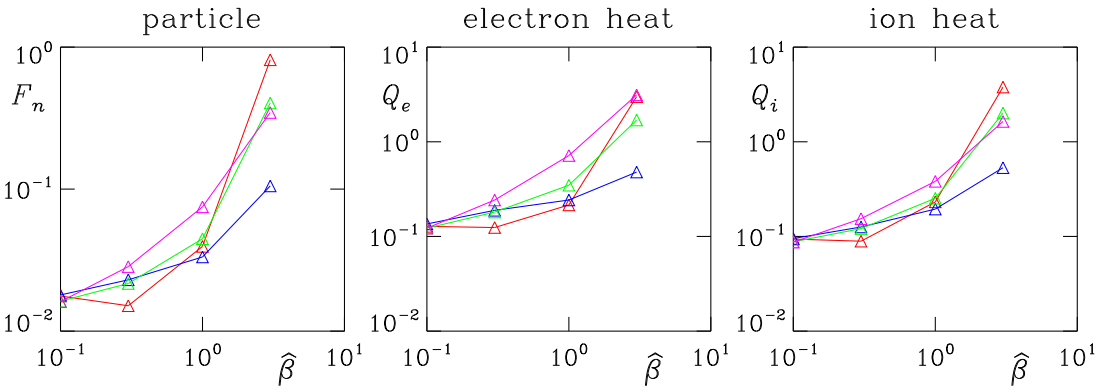

Figure 2: β scaling of the three ExB transport fluxes for low collisionality edge turbulence. The nominal scaling is shown (red), together with the results keeping linear magnetic flutter only (blue), or nonlinear flutter only (green), or without either flutter piece (magenta). Magnetic flutter is stabilizing initially but loses this influence in the relevant regime ($\hat{\beta} > 0.3$) as the nonlinear effects assume dominance, leaving a trend consistent with L-mode transport. Note that this scaling is at constant B, not at constant ρ^*.

finite β. The ballooning character of the electron dynamics is reflected by the larger amplitude and narrower envelope of $\widetilde{\phi}$ compared to $\widetilde{n}_e$ and $\widetilde{T}_i$. This very narrow structure was confirmed by a test run with 4 times the parallel resolution. We therefore find a sort of ITG/kinetic ballooning mode, following the ion and electron mode structure, respectively. These same diagnostics found edge turbulence to have a more drift-wave like character in the electrons.[6, 7] Ballooning is evidently of much more relevance in the core than in the edge. The same is true of electron heat flux transport down disturbed magnetic field lines.

The small value of $\hat{\mu}$ makes the computations very expensive. A series of tests was carried out to see if the extreme mass ratio could be relaxed; values of $\hat{\mu}$ of 0.05, 0.1, and 0.2 were used, corresponding to mass ratios of about 1800, 900, and 450. The ion heat transport Q_i was found to be sensitive to this, as values of 0.854, 0.497, and 0.620 resulted, compared to the nominal 1.49. In each case, the electron heat transport was about $Q_e = 0.6\,Q_i$. The nonmonotonicity of the result reflects a mode structure change as $\hat{\mu}$ approaches unity: for small values of $\hat{\mu}$, the $Q_{i,e}$ values first decrease with increasing $\hat{\mu}$. But for $\hat{\mu} \gtrsim 0.1$, the mode structure begins to acquire a character more reflective of drift waves than of ballooning modes, especially in the relationship between $\widetilde{\phi}$ and $\widetilde{p}_e$ (Fig. 1c). Simulations using reduced mass ratios (e.g., of the order of 10^2) in order to lower the computational requirements will therefore end up with $\hat{\mu}$ values near unity, erroneously recovering results too similar to edge turbulence. Finite β ITG/drift wave turbulence is evidently too subtle and complicated to be consistent with the very simple linear mixing length picture which has resulted from electrostatic computations with adiabatic electrons.

The specific effects of all of the finite β ingredients were also investigated in the context of edge turbulence ($\hat{\beta} = 1$ and $\hat{\mu} = 5$) but with relatively low collisionality ($\hat{\nu} = 1$). The results (see Fig. 2) were much the same as in a similar study done in a gyrofluid model [11]: there is a regime, well below the nominal ideal ballooning stability boundary ($\alpha_M = \hat{s}$), in which the transport rises sharply with β, and the cause of this is found to be specifically the "magnetic flutter" nonlinearity associated with $\nabla_\parallel$. The linear modification of $\nabla_\parallel p_e$ due to $\widetilde{A}_\parallel$ is stabilizing, and is responsible for the falling trend with β in gyro-Bohm units (i.e., with constant ρ^*, not to be confused with the trend with constant-B in an experiment). Runs conducted without either flutter piece found the rising trend discussed in Ref. [5]. At moderate β, the effect of the

nonlinear flutter piece is to cancel the linear one, giving the rising trend. This is accompanied with the mode structure changes noted above. The mode is still properly characterised as ITG, because $\widetilde{T}_i > \widetilde{\phi}$ and is more strongly ballooned (cf. Ref. [6] for these signatures), but since $\widetilde{\phi} > \widetilde{p}_e$ and is in turn more strongly ballooned, the electron part of the system is more ballooning like. Indeed, we find that the contribution due to $\widetilde{p}_e$ in the vorticity dynamics does become larger than that due to $\widetilde{J}_\parallel$, confirming this mode structure.

2. Electron scales

Nonadiabatic electrons also play a role in the dynamics of electron temperature gradient (ETG) modes on much smaller space-time scales. For $\lambda_{De} \lesssim \rho_e$, ITG and ETG modes are perfectly isomorphic in the electrostatic and adiabatic regime. Under these circumstances, it is therefore permissible to transfer linear results from the one to the other by simply interchanging the species labels. In the nonlinear regime, this symmetry is broken, however, due to a subtle difference in the response of the adiabatic species.[12] Whereas in sheared slab geometry, ETG and ITG simulations still saturate at similar normalized levels (consistent with mixing length expectations, $\chi \sim \gamma^{\max}/k_\theta^2 \sim \rho^2 v_t/L_T$), toroidal ETG modes sometimes go to much higher amplitude than their ITG counterpart and exhibit streamers, i.e., radially elongated vortices. This behavior can be interpreted in the framework of secondary instability theory. Depending on the degree of "slabness" (as characterized by the intrinsic parallel velocity component) of linear electrostatic ETG/ITG modes, we find that one of two distinct processes may dominate as nonlinear saturation mechanism.[13] Perpendicular shear in the *parallel* flow of the linear instability drives a strong (hereafter, "Cowley") secondary, described in detail in Ref. [14]. Importantly, this secondary is not sensitive to the form of the adiabatic response and thus leads to the same (mixing-length type) transport level in both slab cases. Predominantly curvature driven modes, on the other hand, are broken up by a secondary (hereafter, "Rogers") instability that is driven by the perpendicular shear in the eigenmode's *perpendicular* $\mathbf{E} \times \mathbf{B}$ flow.[12, 15] Because the Rogers secondary is significantly weakened on ρ_e scales (as compared to ρ_i scales) by the adiabatic ion response, a curvature driven ETG mode tends to saturate at a much higher normalized level than both its ITG counterpart and mixing length expectations. With this enhancement, associated with high-amplitude streamers, ETG-induced transport can be comparable to electron energy transport induced by ITG modes and trapped electron modes.

On the nature of high-amplitude streamers. The single most striking feature in nonlinear ETG simulations (here, we use the gene code which is described in Ref. [12]) is the occurrence of radially elongated vortices with large fluctuation amplitudes in certain parameter regimes.[12] Streamers have been observed both in tokamak [12, 13, 15] and in stellarator [16, 17] simulations if and only if the underlying long-wavelength instabilities have a clear toroidal (*vs.* slab) character. For large aspect ratio tokamaks with circular cross section and small Shafranov shift, this is the case for $\hat{s} \gtrsim 0.4$ and $R/L_{T_e} \gg R/L_{T_e}^{\mathrm{crit}}$.[12] In the presence of streamers, the fluctuation and transport levels can be boosted by more than an order of magnitude with respect to mixing length expectations. Streamer aspect ratios computed via the radial/poloidal autocorrelation functions of $\tilde{\phi}$ are typically of the order of 2.[17] This value seems somewhat low compared with the visual impression and might indicate that refined measurements are called for (i.e., inspired by percolation theory). The dominant modes for Cyclone base case parameters have $k_\theta \rho_e \sim 0.15$ [12, 13] and exibit a phase shift of $\sim \pi/3$ between $\tilde{\phi}$ and $\tilde{T}$ (which is basically equal to that of the corresponding linear streamer).[12] At higher values of k_θ, the spectra exhibit a power law behavior with exponents that seem to be quite universal.[13, 17] The turbulent transport (both with *and* without streamers) is always predom-

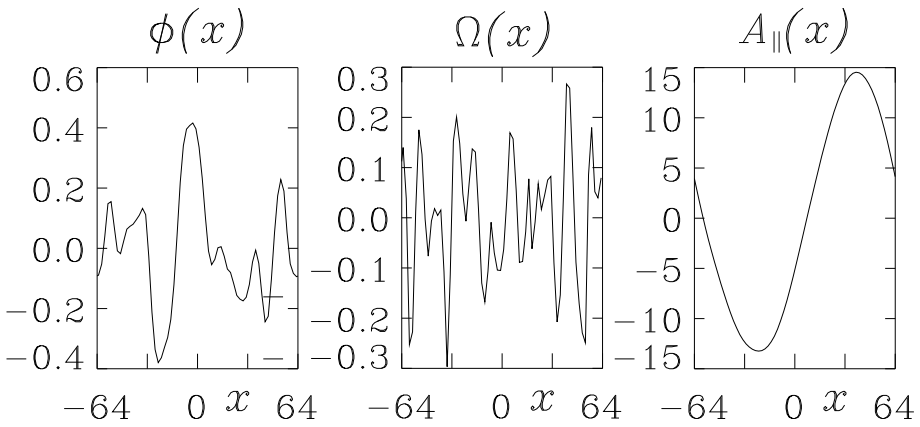

Figure 3: Snapshot of flux surface averaged values of $\tilde{\phi}$, $\tilde{\Omega} \equiv \tilde{v}'_{Ey}$, and $\tilde{A}_\parallel$ as a function of the radial coordinate x (normalized to ρ_e).

inantly electrostatic.[12, 16]

On the role of zonal flows and fields. Zonal flows and fields are purely radial ($k_\theta = k_\parallel = 0$) variations of $\tilde{\phi}$ and $\tilde{A}_\parallel$ associated with $\mathbf{E} \times \mathbf{B}$ flows and magnetic field fluctuations. They can be self-generated by the turbulence and may in turn act as its dominant nonlinear saturation mechanism. But how important are they on ρ_e scales? A typical snapshot of the flux-surface averaged values of $\tilde{\phi}$ and $\tilde{A}_\parallel$ from a stellarator simulation is shown in Fig. 3 together with the $\mathbf{E}\times\mathbf{B}$ shearing rate $\tilde{\Omega} \equiv \tilde{v}'_{Ey}$.[17] In this case, the space and time averaged RMS values of $\tilde{\Omega}$ and and the magnetic shear fluctuation, $\tilde{s} \equiv qR\,\tilde{B}'_y/B$, are given by $\tilde{\Omega}^{\rm rms} \approx 0.12\, v_{te}/R \sim 0.3\,\gamma^{\rm max}$ and $\tilde{s}^{\rm rms} \approx 0.018$ where $\gamma^{\rm max}$ is the maximum linear growth rate. This is in stark contrast to results from ITG turbulence where $\tilde{\Omega}$ can significantly exceed $\gamma^{\rm max}$ (e.g., $\tilde{\Omega}^{\rm max}/\gamma^{\rm max} \sim 14$ in Ref. [18]). In the ITG case, one obtains the zonal flow saturation criterion $\tilde{\Omega}^{\rm rms} \lesssim \gamma^{\rm max}$ only after correcting for the ineffectiveness of the high frequency component of $\tilde{\Omega}$. The zonal components of ETG turbulence contribute only 1% or so to the total $\tilde{\phi}^{\rm rms}$.[17] This is again in contrast to the findings in the ITG case where zonal modes with $k_x\rho_i \sim 0.1$ tend to contribute significantly or even dominate the fluctuation free energy contained in $\tilde{\phi}$ (see, e.g., Ref. [18] and references therein). Moreover, since magnetic shear variations primarily affect the linear growth rates of the ETG modes driving the turbulence [19], a value of $\tilde{s}^{\rm rms} \approx 0.018$ is certainly too small for zonal fields to play a significant role. Similar zonal flow/field saturation levels as the ones reported here have also been found in ETG simulations of tokamak plasmas. Thus, we may conclude that, at least for a significant region in parameter space, zonal modes on ρ_e scales tend to play a subdominant role in the turbulent dynamics. (A possible exception could be the simulation for tokamak edge parameters described in Ref. [20].)

A predictive numerical model for turbulent transport. Building on these results and insights, we now develop an *ab initio* numerical model which is shown to even quantitatively explain the nonlinear gyrokinetic simulation results.[13] The basic idea is to predict the saturation amplitude by balancing primary (γ_ℓ) and secondary ($\gamma_{\rm nl}$) growth rates. To do this, one must first calculate $\gamma_{\rm nl}$. At sufficiently high amplitude, $\gamma_{\rm nl} \propto \tilde{\phi}_\ell$. Using the `gs2` code (see Ref. [12] and references therein), we thus compute $\gamma^0_{\rm nl}$ by freezing a given linear eigenmode at a fiducial high amplitude ($\tilde{\phi}_\ell = \tilde{\phi}^0_\ell$), and using this state as the "equilibrium" for a sequence of initial value calculations with varying k_x. (In the sequel, we consider $k_x/k_y = 0.5$ as a representative value.) Given $\tilde{\phi}^0_\ell$, $\gamma^0_{\rm nl}$ and γ_ℓ, the RMS amplitude of $\tilde{\phi}$ in the turbulent state is estimated by $\tilde{\phi}/\tilde{\phi}^0 = \gamma_\ell/\gamma^0_{\rm nl}$. (We note that all our results are in the strong turbulence regime, where $\chi_e \propto \tilde{\phi}$, so that $\gamma_\ell/\gamma^0_{\rm nl}$ also roughly predicts the anomalous transport coefficient.) Somewhat surprisingly, we find that ETG driven turbulent transport is well described by this relatively simple

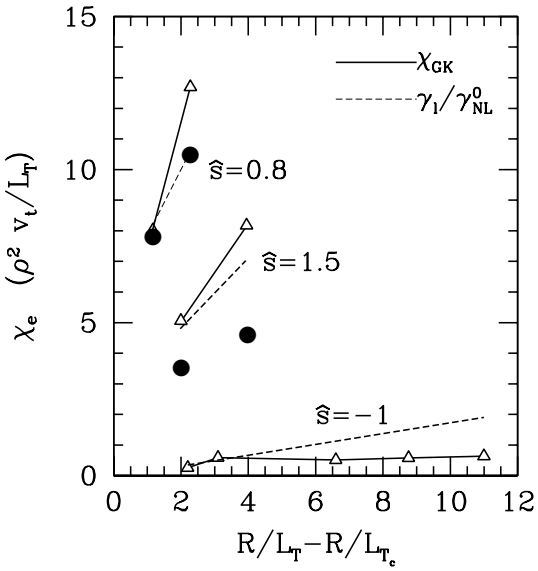

Figure 4: χ_e from nonlinear gyrokinetic ETG simulations [open triangles] for our nominal parameters and $\hat{s} = 0.8$ ($R/L_{T_c} \sim 4.6$), $\hat{s} = 1.5$ ($R/L_{T_c} \sim 7.1$), and $\hat{s} = -1$ ($R/L_{T_c} \sim 6.3$), together with numerical [dashed lines] and semi-analytical [full circles] predictions.

model as can be seen in Fig. 5. Here, the following physical parameters have been used (besides the ones mentioned in the figure itself): $R/L_n = 2.2$, $q = 1.4$, and $\tau_e = 1/\tau_i = T_e/T_i = 1$, corresponding to the "Cyclone base case". A single fit parameter (related to the ratio of the heat flux to $\tilde{\phi}$) was held fixed for all the points in the figure. Importantly, neither the linear growth rate nor the maximal value of $\gamma/\langle k_\perp^2 \rangle$ predicts the variation found in the nonlinear simulations. For example, the negative shear cases with $R/L_{Te} - R/L_{Tc} > 6$ have maximized $\gamma/\langle k_\perp^2 \rangle$ values which *exceed* those of the $\hat{s} = 0.8$ cases. It is the variation of the secondary growth rate as the linear eigenfunction changes in response to the equilibrium parameters that correlates with the difference in the nonlinear flux. The secondary growth rates exhibit a strong dependence on magnetic shear as the secondary transitions from a Rogers secondary (moderate positive shear) to a Cowley secondary (negative shear). The good agreement between gyrokinetic simulation and numerical model encourages us to persue a semi-analytical treatment of the balance between primaries and secondaries, condensing several important pieces of information about the saturated nonlinear state into into simple algebraic formulas.

Towards an analytic theory of ∇T driven turbulence For $\hat{s} \gtrsim 0.4$ and $R/L_n \lesssim R/L_{T_j} \gg R/L_{T_j}^{\rm crit}$, ITG/ETG modes have a predominantly toroidal character and the Rogers secondary is the dominant nonlinear saturation mechanism. The region close to criticality (algebraic expressions for $R/L_{T_j}^{\rm crit}$ in tokamaks and in the stellarator Wendelstein 7-AS have been derived in Refs. [21] and [16], respectively) as well as the low/negative shear region involve the Cowley secondary and are more difficult to treat. This task is left for future work. Using a host of linear gyrokinetic simulations, we find that under these conditions the linear growth rates of long-wavelength ITG/ETG streamers may be well described by the simple algebraic formula

$$\gamma_\ell = \frac{\alpha_1}{\tau_j} \frac{v_{tj}}{L_{T_j}} \left(k_\theta \rho_j - k_\theta^{\rm c} \rho_j\right), \quad k_\theta^{\rm c} \rho_j = \frac{L_{T_j}}{qR} \tau_j^{1/2}, \quad \alpha_1 \approx 0.25\,. \tag{1}$$

Here, finite β and λ_{De} effects have again been neglected. Note that Eq. (6) is independent of $\hat{s}$ and R/L_n. Interestingly, this result can also be derived in the framework of gyrofluid theory. Employing, e.g., the basic model described by Eqs. (1-3) in Ref. [22], and generalizing their Eq. (3) to $\partial_t T + A\,\nabla_\parallel v + \mu A\,|\nabla_\parallel| T = 0$ one gets exactly the above result with $\alpha_1 =$

$2\mu/(1+4\mu^2)$. Using $\mu = (8/\pi)^{1/2}$ as suggested by Hammett *et al.*[23] leads to the prediction $\alpha_1 \approx 0.285$ which is very close to the gyrokinetic result.

The second ingredient in our ETG/ITG turbulence theory is an algebraic formula for the nonlinear growth rates of Rogers secondaries in the presence of a large amplitude linear streamer. (Here, we will focus on the ETG case, the ITG case can be treated in an analogous fashion.) According to Fig. 4 in Ref. [15], its maximum with respect to k_x is given by

$$\gamma_{\rm nl} = \frac{\alpha_2}{\tau_e}\,\frac{v_{te}}{L_{T_e}}\,(k_\theta\rho_e)^4\left[\frac{e\tilde{\phi}}{T_e}\frac{L_{T_e}}{\rho_e}\right] \tag{2}$$

with $\alpha_2 \approx 0.18$. For $\hat{s} \neq 0$, the primary modes twist with the field lines, leading to an increase of the effective k_θ. We will take this effect into account by replacing k_θ^4 in Eq. (8) with $\langle k_\theta^2\rangle^2$ where the angular brackets denote weighting with $|\tilde{\phi}(\theta)|^2 \propto \exp(-\nu\theta^2)$. A good fit formula for ν, inferred from dozens of linear gyrokinetic simulations for $\hat{s} \gtrsim 0.2$ and $R/L_{T_e} \gg R/L_{T_e}^{\rm crit}$, is $\nu = 0.53\,q\,(k_\theta\rho_e) + \max\{0.09, 0.19\,\hat{s}^2\}\,(q/\tau_e)\,(R/L_{T_e})\,(k_\theta\rho_e)^2$.

Having established analytical expressions for the growth rates of primaries and secondaries, we can now explicitly balance the two, $\gamma_\ell = \gamma_{\rm nl}$. In the strong turbulence regime, this yields

$$\chi_e \approx \left[\frac{e\tilde{\phi}}{T_e}\frac{L_{T_e}}{\rho_e}\right]\frac{\rho_e^2 v_{te}}{L_{T_e}} = \frac{0.15}{\tau_e^{3/2}\,(1+\hat{s}^2/2\hat{\nu})^2}\left(\frac{qR}{L_{T_e}}\right)^3\frac{\rho_e^2 v_{te}}{L_{T_e}} \tag{3}$$

after maximization over k_θ where $\hat{\nu}$ is ν taken at $k_\theta^d = 4k_\theta^c/3$. Evaluating this expression for the four points with positive shear shown in Fig. 5, we get surprisingly good agreement. Note that another prediction of this semi-analytical model is that the poloidal length scale of the dominant modes is given by k_θ^d. For Cyclone base case parameters (including $\hat{s} = 0.8$) we get $k_\theta^d \sim 0.13$, in reasonable accordance with nonlinear simulation results, exhibiting $k_\theta^d = 0.15 \pm 0.05$.[12, 13]

An analogous treatment of ITG modes and associated Rogers secondaries leads to the estimate $\chi_i \approx \mathcal{G}(q,\hat{s},\tau_i)\,\rho_i^2 v_{ti}/L_{T_i}$ which is one order down in R/L_T compared to the ETG case, Eq. (15). A scaling like this has indeed been observed in nonlinear simulations of ITG turbulence with adiabatic electrons.[1] Moreover, the prediction $\mathcal{G}(q=1.4, \hat{s}=0.8, \tau_i=1) \sim 2$ is roughly consistent with the simulation results. It should be kept in mind, however, that in contrast to the ETG case, ITG turbulence can be controlled by zonal modes, an effect which is not accounted for by the present theory. This is true, in particular, as the system approaches marginality.

3. Summary

We have investigated the effects of finite β and nonadiabatic electrons, presenting results for both ion and electron space-time scales, and both tokamaks and stellarators. At ion scales, electromagnetic effects through passing electrons are able to completely change the nonlinear mode structure and therefore the qualitative character of the turbulence. An electron-to-ion mass ratio scan at finite β reveals a transition from core-like to more edge-like behavior with decreasing m_i/m_e. This sets serious limits on attempts to reduce the computational effort for two-species simulations by using fake mass ratios. Gyrokinetic simulations of ETG and ITG turbulence show that the linear symmetry between them is nonlinearly broken. This finding can be explained in terms of a secondary instability theory which may also serve as a basis for simple numerical or semi-analytical models. The latter are shown to successfully capture key features of the streamer-dominated turbulent state even quantitatively. This raises hope that more comprehensive analytical theories of temperature gradient driven turbulence might be developed

along those lines. Generally speaking, our results show that the standard interpretation of turbulent transport as some type of isotropic diffusion (random walk) process is not universally applicable.

References

[1] A. M. Dimits, G. Bateman, M. A. Beer *et al.,* Phys. Plasmas **7**, 969 (2000).

[2] M. Wakatani and A. Hasegawa, Phys. Fluids **27**, 611 (1984).

[3] B. Scott, Phys. Rev. Lett **65**, 3289 (1990); Phys. Fluids B **4**, 2468 (1992).

[4] A. B. Mikhailovskii and L. I. Rudakov, Sov. Phys. JETP **17**, 621 (1963).

[5] B. Scott, Plasma Phys. Control. Fusion **39**, 1635 (1997).

[6] B. Scott, New Journal of Physics **4**, 52 (2002).

[7] B. Scott, *Drift wave versus ballooning mode turbulence*, submitted to Phys. Plasmas.

[8] B. Scott, Contrib. Plasma Phys. **38**, 171 (1998).

[9] B. Scott, Phys. Plasmas **5**, 2334 (1998).

[10] B. Scott, Phys. Plasmas **8**, 447 (2001).

[11] P. B. Snyder and G. W. Hammett, Phys. Plasmas **8**, 744 (2001).

[12] F. Jenko, W. Dorland, M. Kotschenreuther, and B. N. Rogers, Phys. Plasmas **7**, 1904 (2000).

[13] F. Jenko and W. Dorland, *Prediction of significant tokamak turbulence at electron gyroradius scales,* to appear in Phys. Rev. Lett.

[14] S. C. Cowley, R. M. Kulsrud, and R. Sudan, Phys. Fluids B **3**, 2767 (1991).

[15] W. Dorland, F. Jenko, M. Kotschenreuther, and B. N. Rogers, Phys. Rev. Lett. **85**, 5579 (2000).

[16] F. Jenko and A. Kendl, New Journal of Physics **4**, 35 (2002).

[17] F. Jenko and A. Kendl, Phys. Plasmas. **9**, 4103 (2002).

[18] T. S. Hahm, M. A. Beer, Z. Lin *et al.,* Phys. Plasmas **6**, 922 (1999).

[19] C. Holland and P. H. Diamond, Phys. Plasmas **9**, 3857 (2002).

[20] F. Jenko and W. Dorland, Plasma Phys. Control. Fusion **43**, A141 (2001).

[21] F. Jenko, W. Dorland, and G. W. Hammett, Phys. Plasmas **8**, 4096 (2001).

[22] M. Ottaviani, M. A. Beer, S. C. Cowley *et al.,* Phys. Rep. **283**, 121 (1997).

[23] G. W. Hammett, W. Dorland, and F. W. Perkins, Phys. Fluids B **4**, 2052 (1992).